Available online at www.sciencedirect.com
SCIENCE DIRECT®
C. R. Chimie 7 (2004) 29–34
COMPTES RENDUS CHIMIE

Preliminary communication / Communication

Synthesis and characterization of the new delafossite-type oxide $CuNi_{1/3}V_{2/3}O_2$

Khadija El Ataoui [a,b], Jean-Pierre Doumerc [b,*], Abdelaziz Ammar [a], Jean-Claude Grenier [b], Patrice Dordor [b], Michel Pouchard [b]

[a] *Laboratoire de chimie du solide minéral, faculté des sciences Semlalia, université Cadi-Ayyad, BP 2390, Marrakech, Maroc*
[b] *ICMCB–CNRS, 87, av. du Docteur-Albert-Schweitzer, 33608 Pessac cedex, France*

Received 22 July 2003; accepted after revision 29 September 2003

Abstract

Whereas neither delafossite-type $Cu^{I}V^{III}O_2$ nor $Cu^{I}Ni^{III}O_2$ exist, the authors have succeeded in preparing the delafossite oxide $Cu^{I}Ni^{II}_{1/3}V^{III}_{1/3}V^{IV}_{1/3}O_2$, using classical solid-state reaction. The most probable formal oxidation state for nickel is II, while for vanadium it is a mixed state +III/+IV. The predominant magnetic interactions are antiferromagnetic, but no evidence could be found for long-range ordering. Charge transport results from a hopping process involving V^{3+} and V^{4+} cations. As XRD did not reveal any cation ordering, the observed $T^{-1/4}$-dependence of the electrical conductivity (Mott's law) is ascribed to a random distribution of the relevant sites. ***To cite this article: K. El Ataoui et al., C. R. Chimie 7 (2004)***.

Résumé

Alors que, ni $Cu^{I}V^{III}O_2$, ni $Cu^{I}Ni^{III}O_2$ de type delafossite n'existent, les auteurs ont pu préparer l'oxyde delafossite $Cu^{I}Ni^{II}_{1/3}V^{III}_{1/3}V^{IV}_{1/3}O_2$, par réaction classique dans l'état solide. Le degré d'oxydation formel le plus probable pour le nickel est II, alors que pour le vanadium il est intermédiaire entre III et IV. Les interactions magnétiques prépondérantes dans cet oxyde sont antiferromagnétiques, mais aucune preuve de l'existence d'un ordre à longue distance n'a été obtenue. Le transport de charges résulte d'un processus de saut impliquant des cations V^{3+} et V^{4+}. Comme la diffraction X ne révèle aucun ordre cationique, la variation en $T^{-1/4}$ de la conductivité électrique (loi de Mott) est attribuée à une répartition aléatoire des sites concernés. ***Pour citer cet article : K. El Ataoui et al., C. R. Chimie 7 (2004)***.

Keywords: Delafossite; Magnetic properties; Electrical properties; Variable-range hopping; $CuNi_{1/3}V_{2/3}O_2$

Mots clés : Delafossite ; Propriétés magnétiques ; Propriétés électriques ; *Variable-range hopping* ; $CuNi_{1/3}V_{2/3}O_2$

* Corresponding author.
E-mail address: doumerc@icmcb.u-bordeaux.fr (J.-P. Doumerc).

doi:10.1016/j.crci.2003.09.009

1. Introduction

A renewed interest for $CuFeO_2$ delafossite-type oxides has been observed in the last few years. The reason is that, in addition to previously mentioned applications of these materials such as catalysis [1], new areas seem to be concerned such as transparent p-type conductors [2] and thermoelectric conversion [3]. The delafossite structure also provides triangular lattices appropriate for investigating frustrated magnetic systems [4]. From the point of view of crystal chemistry, we have recently shown that, although $CuVO_2$ does not exist, V^{+III} can be stabilized in the delafossite networks of $CuFe_{1-x}V_xO_2$ solid solutions [5]. This shows that a delafossite solid solution can be prepared even when one of the end members does not exist. The case of the $CuNi_{1-x}V_xO_2$ compositions is interesting, since $CuNiO_2$ does not have a delafossite-type structure, but exhibits a rocksalt-related structure in which copper is divalent instead of being monovalent, which is actually required for stabilizing the delafossite structure.

2. Sample preparation

Polycrystalline samples of nominal compositions $CuNi_{1-x}V_xO_2$ with x = 1/3, 1/2 and 2/3 were prepared by heating stoichiometric mixtures of Cu, CuO (Merck, 99.9%), NiO (Strem Chemicals, 99.99%) and V_2O_5 (Schüchardt München, 99.8%) in an evacuated silica tube. Experimental conditions and reaction product compositions, determined by XRD analysis, are summarized in Table 1.

Only for x = 2/3 a single phase was obtained. Its stability in air was studied by TGA. Fig. 1 shows that, at a heating rate of 110 K per hour, weight uptake starts at 450 K and that the oxidation process is complete at 650 K. Assuming that the oxidized material contains divalent copper, divalent nickel and pentavalent vanadium, the theoretical weight gain should be of 10.72%. The experimental value (9.5%) is slightly smaller. At least three effects can account for this discrepancy. First the oxidized products can be oxygen-deficient, as it is well known for V^{+V} oxides. Second oxygen can be intercalated into the starting delafossite network. However, this latter effect should be limited as, first, the synthesis is carried out in an evacuated sealed ampoule and, secondly, the lattice constant a is not large enough to allow large amounts of intercalated oxygen, like, for instance, in rare-earth delafossites [6]. The third effect could be an unexpected very weak deviation of the Cu/Ni/V ratios from 3/1/2, such as, for example, a Ni/V ratio slightly larger than 1/2.

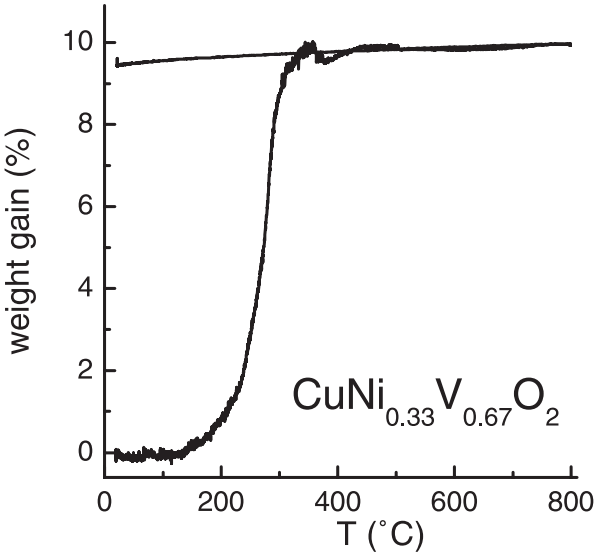

Fig. 1. TGA of $CuNi_{1/3}V_{2/3}O_2$ under oxygen. Heating rate: 110 °C h^{-1}.

Table 1
Conditions for sample preparation

x-Value in $CuNi_{1-x}V_xO_2$	Starting mixture	Reaction temperature (K)	Reaction time (h)	Colour of reaction product	Reaction products
1/3	3 Cu + 3 CuO + 4 NiO + V_2O_5	870, 970	24	dark green	$Ni_3V_2O_8$ + Cu_2O + NiO
1/2	CuO + 3 Cu + 2 NiO + V_2O_5	870, 920, 970, 1 070	12, 24	orange–yellow	delafossite phase + $Ni_3V_2O_8$ + Cu_2O + NiO
2/3	3 Cu + NiO + V_2O_5	920, 970	24	black	single delafossite phase

Table 2
Conditions for powder XRD data collection and Rietveld refinement of $CuNi_{1/3}V_{2/3}O_2$ in $R\bar{3}m$ space group (No. 166)

Diffractometer	Philips X'Pert MPD
Radiation	Cu Kα
Temperature	RT
2θ range (°) ; step (°) ; counting time (s)	5–120; 0.02; 19
Rietveld program	Fullprof [7]
Profile function	pseudo-Voigt
Number of reflections	41
Number of fitted parameters	16
R_p [a]	0.030
R_{wp} [a]	0.046
Conventional R_p [b]	0.18
Conventional R_{wp} [b]	0.14
R-Bragg	0.057
χ^2	5.6

[a] *R*-factors not corrected for background.
[b] Conventional Rietveld *R*-factors corrected for background.

3. Structural characterization

Powder XRD data of $CuNi_{1/3}V_{2/3}O_2$ were collected using the experimental conditions given in Table 2.

Cell and structural parameters were refined using the Rietveld method. Program reference [7] and refinement conditions are also mentioned in Table 2. Crystal system, space group, lattice constants and other crystallographic and structural data are given in Table 3.

The refinement procedure finally provided the atomic positions and the isotropic thermal parameters reported in Table 4. Experimental and calculated diffractograms are displayed in Fig. 2.

Interatomic distances are given in Table 5.

The Cu–O distance (1.82 Å) is in good agreement with the sum of ionic radii (1.84 Å) assuming CN = 2 for Cu^+ (0.46 Å) and CN = 4 for O^{2-} (1.38 Å) [8]. As no superstructure peak was observed, we shall assume, in this preliminary report, that the Ni and V atoms are randomly distributed (neutron diffraction experiments are planned to verify this assumption). In these conditions, the M–O distance (2.02 Å) leads to an average ionic radius of 0.64 Å for M-atoms (taking $r^{IV}_{O^{2-}} = 1.38$Å from the Shannon table as oxygen is fourfold coordinated [8]). This value can be compared to two formal hypotheses concerning the oxidation states of Ni and V either $Ni^{2+} + V^{4+} + V^{3+}$ or Ni^{3+}(LS) + 2 V^{3+}. The possibility of Ni^{3+}(HS) is discarded as the HS state was never found in such a D_{3d} site [9]. In the first case, the average ionic radius would be 0.637 Å and in the second case 0.613 Å. The comparison with the experimental value of 0.64 Å is in favour of the first hypothesis, which is the one expected if we consider that the redox equilibrium:

(1) $Ni^{2+}+V^{4+}+V^{3+} \leftrightarrow Ni^{3+}(LS)+2V^{3+}$

is strongly shifted towards the left-hand side. As we shall see below, magnetic measurements including EPR did not provide any evidence about this point. Heavier techniques such as XAS could possibly help solving this problem.

Table 3
Crystallographic data of $CuNi_{1/3}V_{2/3}O_2$

Crystal system	rhombohedral
Space group	$R\bar{3}m$ (N° 166)
Z	3
a (Å) (hexagonal cell)	2.9865(2)
c (Å) (hexagonal cell)	17.191(1)
Unit cell volume (Å^3) (h.c.)	132.79
Molar mass (g mol^{-1})	149.08
Calculated density (g cm^{-3})	5.59
Measured density (g cm^{-3})	5.57

Table 4
Atomic position parameters for $CuNi_{1/3}V_{2/3}O_2$

Atom	Multiplicity and Wyckoff site	*x*	*y*	*z*	*B* (A^2)	Fractional occupancy
Cu	3a	0	0	0	1.1(2)	1
Ni	3b	0	0	1/2	0.7(2)	1/3
V	3b	0	0	1/2	0.7(2)	2/3
O	6c	0	0	0.106(1)	1.5(4)	1

4. Magnetic and electrical properties

Magnetic measurements were performed between 4 and 300 K with a SQUID equipment.

The sample was first cooled in a zero magnetic field (ZFC); the magnetization was measured upon increasing temperature, under 1 T, and then decreasing it (FC). No difference was observed between the two curves. The temperature dependence of the reciprocal molar susceptibility is given in Fig. 3. A linear variation is observed between 200 and 300 K. Fitting with a Curie–Weiss law leads to a molar Curie constant $C_M = 0.86$ (emu) and a Weiss parameter $\theta_p = -80$ K. The theoretical spin-only value expected is 0.792 for the two hy-

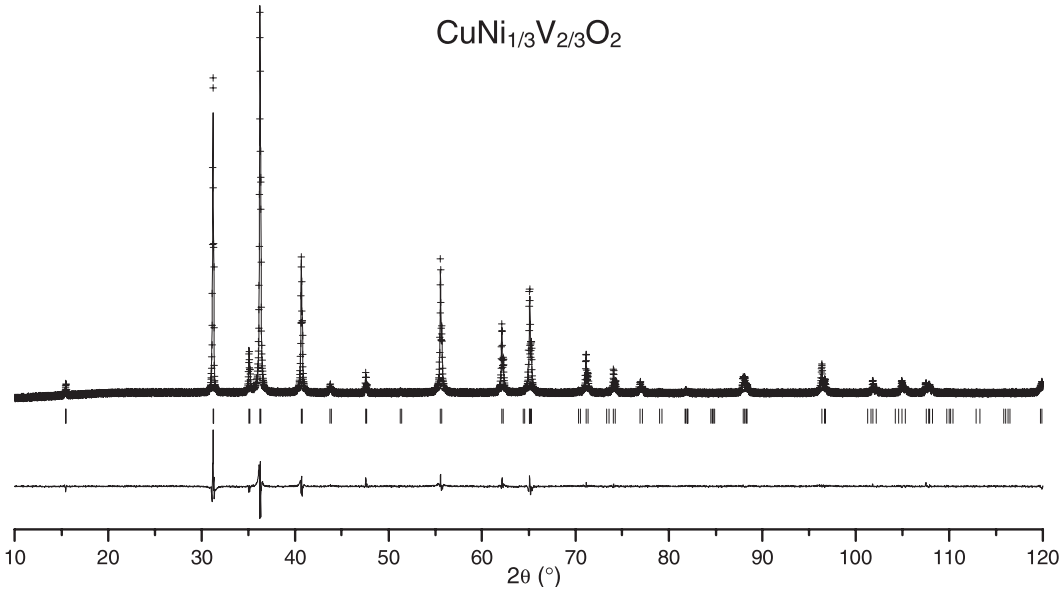

Fig. 2. Measured (discrete points) and calculated (solid line) XRD intensities and their difference for $CuNi_{1/3}V_{2/3}O_2$, at room temperature. Peak positions are indicated by vertical lines.

potheses illustrated by each side of equilibrium (1). We note that the hypothesis in which trivalent nickel would be in a high-spin state would lead to a spin only C_M value of 1.292 and hence can be ruled out in agreement with previous studies [9]. The negative θ_p value reveals that dominant magnetic interactions are antiferromagnetic (AF). However, the behaviour of the reciprocal susceptibility appears rather unusual with respect to that of the previously investigated delafossite oxides containing a single trivalent transition element [10]. The 2D character of the structure generally leads to a minimum in the temperature dependence of the reciprocal susceptibility. This more or less broad minimum is due to short-range spin ordering or spin fluctuations. Instead, in $CuNi_{1/3}V_{2/3}O_2$, the reciprocal susceptibility decreases more rapidly than what is predicted by the Curie-Weiss law. Accounting accurately for such a behaviour would require an appropriate modelling of the system in which at least three types of nearest neighbour interactions should be taken into account, provided that trivalent nickel and vanadium would coexist: V–V, Ni–Ni, and V–Ni interactions. In the other hypothesis, six different types of interactions are theoretically possible and the mixed valence $V^{3+/4+}$ could also give rise to a mechanism of double exchange. Anyway, no long-range ferro- or ferrimagnetic ordering takes place, as the susceptibility does not diverge at a finite temperature. Whether an AF long-range order occurs at low temperature cannot simply be deduced from the present results. We made an attempt to clarify this point using X-band EPR. Unfortunately, the material is EPR silent at room temperature

Table 5
Main interatomic distances (Å) and bond angles (°) in $CuNi_{1/3}V_{2/3}O_2$

Cu–O	×2	1.82(2)		$O–(Ni,V)^{ii}–O^{i}$	95.6(4)
$(Ni,V)^{ii}–O$	×6	2.02(1)		$O–(Ni,V)^{ii}–O^{iv}$	84.4(8)
$O–O^{i}$	×6	2.9865(2)		$Cu–O–(Ni,V)^{ii}$	121.2(6)
$O–O^{iv}$	×3	2.71(2)		$(Ni,V)^{ii}–O–(Ni,V)^{iii}$	95.6(4)
Symmetry code	none	x	y	z	
	i	x	$y-1$	z	
	ii	$x+1/3$	$y+2/3$	$z-1/3$	
	iii	$x+1/3$	$y-1/3$	$z-1/3$	
	iv	$x+2/3$	$y+2/3$	$1/3-z$	

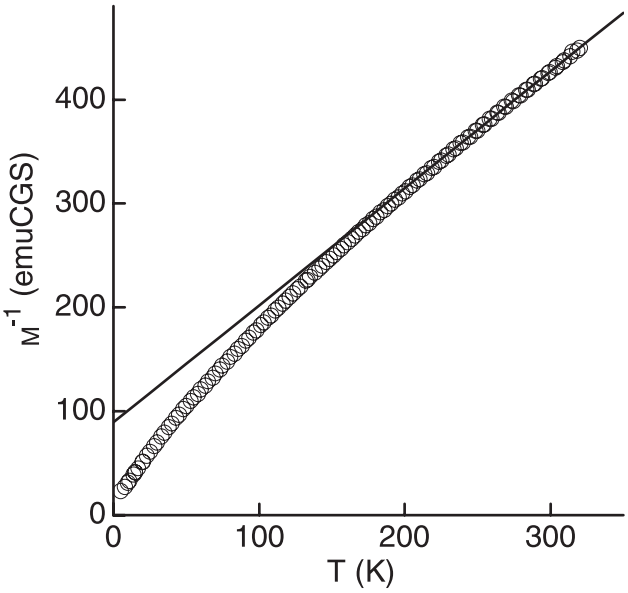

Fig. 3. Temperature-dependence of the reciprocal magnetic susceptibility of $CuNi_{1/3}V_{2/3}O_2$.

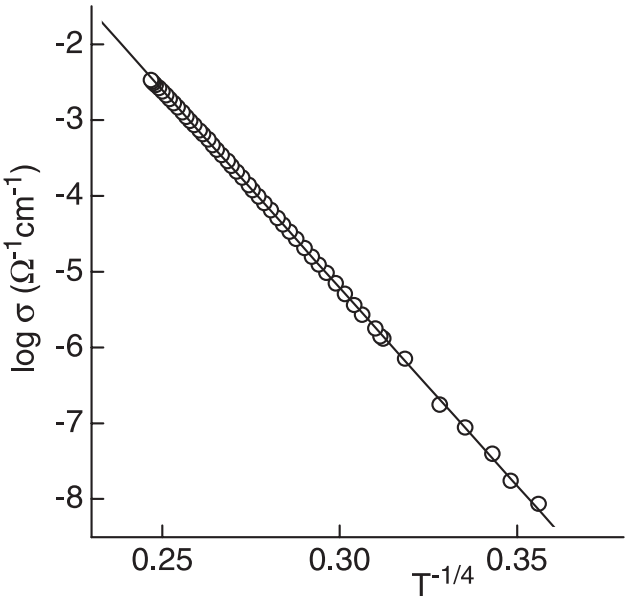

Fig. 4. Logarithm of the electrical conductivity of $CuNi_{1/3}V_{2/3}O_2$ vs. $T^{-1/4}$.

and only an extremely weak signal is detected at 4 K. The absence of signal at room temperature, at first sight, could rule out the presence of LS Ni^{3+} (and hence V^{3+}), which gives a large broad signal in $AgNiO_2$ [9]. However, we have observed that in $CuM_{1-x}V_xO_2$ (M = Cr, Fe), the presence of V^{3+} kills the signal expected from the other transition element. At the present time, we do not understand well this effect and its explanation will require further studies. One possible reason would originate from either dynamic charge fluctuations or dynamic spin fluctuations.

The electrical conductivity is thermally activated, but does not follow an Arrhenius law. It can be fitted according to $\sigma = \sigma_0 \exp(-B/T^n)$ with $n = 0.26$. This n value is very close to 1/4, a value that was predicted by Mott for the case where the prevailing conduction mechanism is variable-range hopping (VRH) and electron–electron correlations are not taken into account [11]. The logarithm of the electrical conductivity is plotted as a function of $T^{-1/4}$ in Fig. 4, showing the expected linear dependence over the whole temperature range in which the measurements were carried out.

5. Discussion

The only pure sample that could be synthesized in the system $CuNi_{1-x}V_xO_2$ is $CuNi_{1/3}V_{2/3}O_2$. On the basis of the bond-length arguments given above, we suggest that nickel is divalent and that vanadium is in a +III/+IV mixed valence state. This assumption is supported by the consideration that Ni^{3+} is strongly oxidizing with respect to V^{3+}.

The nickel and vanadium atoms occupy a flattened octahedron undergoing a D_{3d} distortion that splits the degenerate t_{2g} orbitals into a more stable orbital singlet, a_1, and two degenerate e orbitals at a higher energy. Assuming 1.5 electrons per vanadium atom, the a_1 band is half occupied and the e band is one eights occupied. As the electron density of the a_1 orbital is rather located out of the M layer, the a_1 band should be rather narrow and the corresponding electrons are localized. The opposite holds for the e band. However, two effects should limit its bandwidth W_e. The first one is the 2D character of the structure and the second one is the dilution effect, as one third of the vanadium atoms is replaced by nickel. As no metallic behaviour is experimentally observed, we may conclude that the bandwidth is not large enough to overcome the correlation effects. The resulting state, especially when one deals with cations of d^1 and d^2 configurations, is generally unstable with respect to the formation of metal–metal bonds. XRD did not reveal any superstructure that could have accounted for an ordered arrangement of such pairs. However, pairs can be randomly distrib-

uted and move via an activated electron hopping process. The picture is strongly supported by the observation of the Mott $T^{-1/4}$-behaviour for the electrical conductivity as the VRH mechanism is observed when disorder creates a modulation of the potential energy at the available sites [11].

6. Conclusion

Whereas neither delafossite-type $CuVO_2$ nor $CuNiO_2$ exist, we succeeded in preparing $CuNi_{1/3}V_{2/3}O_2$ using classical solid-state reaction. The most probable formal oxidation state for nickel is II, while for vanadium it is a mixed state +III/+IV, as can simply be anticipated from the strong oxidizing character of Ni^{3+} and the strong reducing character of V^{3+}. Nevertheless, this should be confirmed, and more sophisticated methods than those used up to now are needed. Although it can be clearly stated that the predominant magnetic interactions are antiferromagnetic, an accurate modelling of the magnetic behaviour still requires further investigations. Actually, the edge sharing (MO_6) octahedron triangular network leads to weak superexchange interactions as the M–O–M angle is close to 95.6° and favours frustration effects. In addition, a double exchange mechanism associated with electron hopping from V^{3+} to V^{4+} cations – more or less randomly distributed – could also play a part in the magnetic behaviour. At this stage of the study, this hopping process is considered to be the main cause of the charge transport observed in the oxide and accounts for the $T^{-1/4}$-dependence of the electrical conductivity.

Acknowledgements

We acknowledge technical assistance from Joël Villot (density measurements), Philippe Dagault (TGA), Rodolphe Decourt (resistivity measurements). We also thank Dr. J.-M. Bassat for help with EPR measurements, and Profs G. Villeneuve and P. Gravereau for helpful discussions.

References

[1] J.R. Monnier, M.J. Hanrahan, G. Apai, J. Catal. 92 (1985) 119.
[2] H. Kawazoe, M. Yasukawa, H. Hyodo, M. Kurita, H. Yanagi, H. Hosono, Nature 389 (1997) 939.
[3] H. Yagi, W. Seo, K. Koumoto, Key Eng. Mater. 180–182 (2000) 251.
[4] A.P. Ramirez, R. Jager-Waldau, T. Siegrist, Phys. Rev. B 43 (1991) 10461.
[5] K. El Ataoui, J.-P. Doumerc, A. Ammar, P. Gravereau, L. Fournès, A. Wattiaux, M. Pouchard, Solid-State Sci. 5 (2003) 1239.
[6] R.J. Cava, H.W. Zandbergen, A.P. Ramirez, H. Takagi, C.T. Chen, J.J. Krajewski, W.F. Peck Jr, J.V. Waszczak, G. Meigs, R.S. Roth, L.F. Schneemeyer, J. Solid-State Chem. 104 (1993) 437.
[7] J. Rodriguez-Carvajal, FULLPROF version 1.9c, May 2001, LLB (unpublished).
[8] R.D. Shannon, Acta Crystallogr. A 32 (1976) 751.
[9] A. Wichainchai, P. Dordor, J.-P. Doumerc, E. Marquestaut, M. Pouchard, P. Hagenmuller, A. Ammar, J. Solid-State Chem. 74 (1988) 126.
[10] J.-P. Doumerc, A. Wichainchai, A. Ammar, M. Pouchard, P. Hagenmuller, Mat. Res. Bull. 21 (1986) 745.
[11] N.F. Mott, E.A. Davis, Electronic processes in non-crystalline materials, 2nd ed, Clarendon Press, Oxford, UK, 1979, p. 32.